Partial shell-filled core-shell tecto(dendrimers): A strategy to surface differentiated nano-clefts and cusps

Donald A. Tomalia*†, Herbert M. Brothers II‡, Lars T. Piehler§, H. Dupont Durst¶, and Douglas R. Swanson*

*Dendritic Nanotechnologies Limited, Central Michigan University, Park Library, Mount Pleasant, MI 48859; ‡Dow Corning Corporation, Midland, MI 48686; §Army Research Laboratory, Aberdeen Proving Ground, MD 21005; and ¶U.S. Army Edgewood Research, Development, and Engineering Center, Aberdeen Proving Ground, MD 21010

Edited by Jack Halpern, University of Chicago, Chicago, IL, and approved February 6, 2002 (received for review December 19, 2001)

Poly(amidoamine) (PAMAM) dendrimer shell reagents possessing either nucleophilic (i.e., primary amines) or electrophilic (i.e., carboxymethyl esters) functional groups have been covalently assembled around appropriate electrophilic or nucleophilic dendrimer core reagents to produce partial shell filled/core-shell tecto(dendrimers). Partial shell-filled products with saturation levels ranging from 28% to 66% were obtained. These metastable, remarkably monodispersed assemblies possess functionally differentiated nano-cusps and clefts that exhibit ''autoreactive'' behavior. Pacification of these autoreactive products with appropriate alkanolamine reagents produced robust, nonreactive, ''hydroxy-amine-differentiated'' surfaces that exhibit very active self-assembly properties. Based on the monodispersity, dimensional scaling, and electrophoretic similarities of PAMAM dendrimers to globular proteins, these assemblies may be viewed as crude biomimetics of classical core shell-type protein aggregates. These dimensionally larger, but analogous PAMAM core-shell tecto(dendrimer) architectures extend and complete a similar pattern of autoreactivity and pacification that was observed earlier for traditional mono PAMAM dendrimer core-shell modules possessing unsaturated shell levels.

Much of the ''ordered complexity'' in our universe can be attributed to self-assembly (1–5) and various forms of suprachemistry (6, 7). The prime prerequisites for these phenomena are appropriate quantized building blocks and suitable geometric/spacial-electrostatic/amphiphilic relationships. Nature has used these parameters over the past few billion years to construct a rich hierarchy of ordered complexity. For the chemist, this hierarchy stretches from the minimalist self-assembly of picoscale building blocks leading to atoms, progressing upwardly, to structure-controlled nano- and μm-sized atom arrays leading to proteins, DNA, membranes, biological cells, and the ultimate complexities of life (8).

Understanding critical rules and patterns associated with these parameters has become a significant driving force in the quest for new synthetic routes to higher-ordered complexity (9, 10). Such abiotic self-assemblies presently reside in three major categories as a function of size-scaled dimensions: (I) supraatomic, (II) supramolecular, and (III) supramacromolecular (Fig. 1) (11).

Since the emergence of dendrimer technology in the early 1980s (12, 13), assembly of reactive monomers (14), branch cells (15, 16), or dendrons (17) around atomic or molecular cores to produce dendrimers according to divergent/convergent dendritic branching principles has become well demonstrated (13, 18). Such systematic filling of space around cores with branch cells as a function of generational growth stages (branch shells) to give discrete quantized bundles of mass has been shown to be mathematically predictable (19, 20) and confirmed by MS (21–24), gel electrophoresis (25, 26), and other analytical methods (25–27).

Access to this level of macromolecular structure control has created substantial interest in the use of dendrimer structures as unimolecular mimics of micelles (11, 28, 29), globular proteins (30, 31), and a variety of other biological self-assemblies (32). Dendrimers have exhibited both endo- and exo-type receptor properties (28, 29, 33) as unimolecular micelle mimics (11, 34, 35). More recently, amphiphilic dendrimers have led to a new and extensive area of supramacromolecular assemblies, which have been reviewed elsewhere (34, 36). As shown in Fig. 1, it is now possible to probe suprachemistry beyond the size of traditional small molecules (i.e. $>$1 nm) with abiotic macromolecular self-assemblies that both mimic and approach the dimensions of biological systems.

Biological systems have evolved successful strategies for synthesizing a wide variety of precise nanostructures. This is evident in the routine biological production of proteins, viruses, cellular organelles, and other assemblies that possess dimensions transcending the entire nanoscale region (7, 8). In many cases, simple proteins ranging in diameters of 1 to 10 nm are used as construction modules for the self-assembly of well-defined, but more complex, protein clusters (aggregates). For example, it is well known that synthesis of the biocatalytic pyruvate dehydrogenase complex involves a sequential assembly of three different-sized globular protein modules (7). This self-assembly process generates a well-defined, surface differentiated, core-shell type nanostucture with a diameter of $\cong$300 nm as shown in Fig. 2. These multienzyme complexes are distinguished by a multitude of surface differentiated, nano-cleft/cusp surface features that are inherent and undoubtedly functional to these structures.

Using strictly abiotic methods, it has been widely demonstrated over the past decade that dendrimers (13) can be routinely constructed with control that rivals the structural regulation found in biological systems. The close scaling of size (30, 33), shape, and quasi-equivalency of surfaces (37–39) observed between nanoscale biostructures and various dendrimer families/generational levels is both striking and provocative (30, 40). These remarkable similarities suggest a broad strategy based on rational biomimicry as a means for creating a repertoire of structure-controlled, size-variable, and shape-variable dendrimer assemblies. Successful demonstration of such a biomimetic approach could provide a versatile and powerful synthetic strategy for systematically accessing virtually any desired combination of size, shape, and surface in the nanoscale region. This would be possible by combinatorial variation of dendrimer module parameters such as (*i*) families (interior compositions), (*ii*) surfaces, (*iii*) generational levels, or (*iv*) architectural shapes (i.e. spheroids, rods, etc.).

The focus of this work is to report recent progress involving the random, inefficient parking of dendrimer shell reagents on a targeted dendrimer core reagent as a strategy for producing partial shell-filled/core-shell tecto(dendrimers) (PS:CST).

This paper was submitted directly (Track II) to the PNAS office.

Abbreviations: PS:CST, partial shell-filled/core-shell tecto(dendrimers); SS:CST, shell saturated/CST; PAMAM, poly(amidoamine); AFM, atomic force microscopy; MALDI-TOF, matrix-assisted laser desorption ionization–time of flight; [EDA], ethylenediamine core; SEC, size exclusion chromatography; MW, molecular weight; EA, 2-aminoethanol; G, generation.

†To whom reprint requests should be addressed. E-mail: tomalia@dnanotech.com.

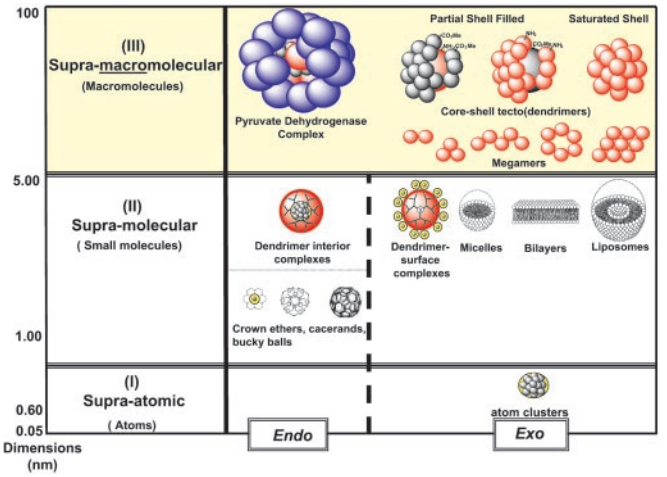

Fig. 1. Supracategories as a function of size scale dimensions (nm): (I) supraatomic, (II) supramolecular, and (III) supramacromolecular.

These abiotic structures are remarkably monodispersed assemblies that may be viewed as unique topological mimics of well-known protein aggregates much as illustrated by pyruvate dehydrogenase complexes (Fig. 2) (7, 41).

Materials and Methods

Structure Ideality and Monodispersity of Dendrimer Reagents. All amine- and carboxymethyl ester-terminated poly(amidoamine) (PAMAM) dendrimers [i.e., ethylenediamine core [EDA]-*dendri*-PAMAM-$(NH_2)_n$ and [EDA]-*dendri*-PAMAM-$(CO_2Me)_n$] used as core and shell reagents were synthesized by standard methods as described (12, 42, 43). These dendrimer reagents were analyzed by H^1/C^{13}-NMR (44), size exclusion chromatography (SEC) (45), atomic force microscopy (AFM) (46), PAGE (25, 26), and matrix-assisted laser desorption ionization–time of flight (MALDI-TOF) MS (21, 24). NMR spectroscopy (H^1/C^{13}-NMR) and MALDI-TOF MS were used to appraise the structural ideality of the [EDA] PAMAM dendrimer reactants. The structural ideality was determined to be between 99% and 87% for generation (G) = 1–7, respectively. Fig. 3 shows the level of mono-dendrimer structural ideality by comparing experimental molecular weight (MW) to theoretical for PAMAM dendrimer, G = 5 (≅ 90.2%). Fig. 4 illustrates typical MS analyses for [EDA] PAMAM dendrimers (G = 1–10). It demonstrates such structure ideality prevails through G = 7 after which the onset of de Gennes dense packing (9, 20, 47) causes moderate to significant mass defects in the higher generations (i.e., G = 8–10) (Fig. 4). A comparison of mono-dendrimer to dimer content is also shown in Fig. 3 (i.e. ≅ 92.4%). The monodispersities based on a comparison of mono-dendrimer versus dendrimer oligomers were 99% to 91% for G = 1–7, respectively. These values were corroborated by parallel PAGE analyses, which allow an appraisal of mono versus dimer (oligomer) content.

Structural notations describing these core-shell structures is an extension of nomenclature used to describe the traditional PAMAM dendrimer reactants (43, 48). For example, consider a dendrimer-core reagent, such as [EDA], G = 5, amine-terminated PAMAM dendrimer [i.e., [EDA]-*dendri*-PAMAM-$(NH_2)_{128}$] reacted with a PAMAM dendrimer shell reagent, G = 2.5, carboxymethyl ester-terminated [i.e., [EDA]-*dendri*-PAMAM-$(CO_2Me)_{32}$]. The expected product after amidation of the terminal groups, to produce a core-shell tecto(dendrimer) would be designated as follows: [[EDA]-*dendri*-PAMAM-$(NH_2)_{128}$]-*amide*-{[EDA]-*dendri*-PAMAM-$(CO_2Me)_{32}\}_n$, where *n* denotes the number of G = 2.5; PAMAM shell reagents that are covalently bonded to a G = 5 PAMAM core reagent.

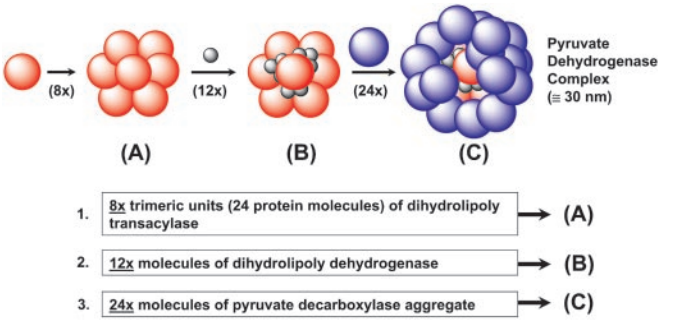

Fig. 2. Sequential self-assembly of three different globular proteins to produce core-shell protein aggregates possessing differientiated nanoscale clefts and cusps.

Alternatively, a shorthand notation may be used for this structure, which is designated as follows: [[EDA];PAMAM, G=5; -(NH_2)]-*amide*-{[EDA]; PAMAM, G = 2.5; -$(CO_2Me)\}_n$.

Analytical Methods

MALDI-TOF Mass Spectrometer Conditions for PAMAM Dendrimers and Core-Shell Tecto(Dendrimers). A stock solution of the dendrimer reagent or core-shell tecto(dendrimer) is prepared by dissolving 3–5 mg of material in methanol. A 1-μl aliquot of the stock solution is mixed with 9 μl of matrix solution. The matrix solution consists of 10 mg/ml 2,5-dihydroxybenzoic acid in 20:80 acetonitrile/water containing 0.1% trifluoracetic acid. The dendrimer/matrix mixture is spotted on the target plate (1 μl/spot) and the solvent is allowed to evaporate under ambient conditions. Analysis is performed with a ThermoBioanalysis Vision 2000 mass spectrometer (Schaumburg, IL) operating in the reflector mode. The value of the laser power setting is generally set between the value where matrix ions first appear and 110% of that value. A typical MALDI-TOF-MS obtained for [EDA]-*dendri*-PAMAM(G = 5)-$(NH_2)_{128}$ is illustrated in Fig. 3. Similar mass spectra were obtained for all PAMAM dendrimer reactants (G = 1–9) and PS:CST products reported in this work, as well as previously reported shell saturated/CST (SS:CST) (48).

SEC. The core-shell tecto(dendrimer) samples (1–8) were dissolved in water and passed through a 0.2-μm syringe-filter (Whatman Anotop 25). They were then injected into a SEC system consisting of a Waters 510 HPLC pump (Milford, MA) a TSK precolumn followed by three analytical columns (G4000PW, G3000PW, and G2000PW) equipped with a Wyatt (Santa Barbara, CA) Refracting Index dual detector (Santa Barbara, CA) at 30°C (run time 40 min). The mobile phase was 0.5M acetic acid/0.5 M sodium nitrate in water. The MWs and MW distributions were obtained by comparing directly to standard PAMAM dendrimer samples (i.e. G = 0–10).

PAGE. General conditions and techniques used for MW analysis by this method are as published (25) and more recently reviewed (26).

Synthesis: Route I—Reaction of [[EDA];PAMAM,G = 5.0;-(NH_2)] with Excess {[EDA];PAMAM,G = 2.5-$(CO_2$ Me)} → [D_c-5Y]-*amide*-{D_s-2.5Z}$_n$; Compound 2. *Autoreactive (PS:CST) product.* To a 10 ml one neck round bottom flask containing a stir bar was added [EDA]-*dendri*-PAMAM, G = 2.5;-$(CO_2Me)_{32}$, (2.0 g, 3.3×10^{-4} mol, 100 equivalent per G = 5), 4 ml of MeOH and lithium chloride (6.0 mg, 1.4×10^{-3} mol, 4 equivalent per G = 2.5). To this stirred mixture was added dropwise [EDA]-*dendri*-PAMAM, G = 5.0-$(NH_2)_{128}$ (95 mg, 3.3×10^{-6} mol) in 2 ml of MeOH over 2 min with stirring. This mixture was sealed under N_2 and heated at 40°C for 25 days. Analysis of an aliquot of the reaction mixture

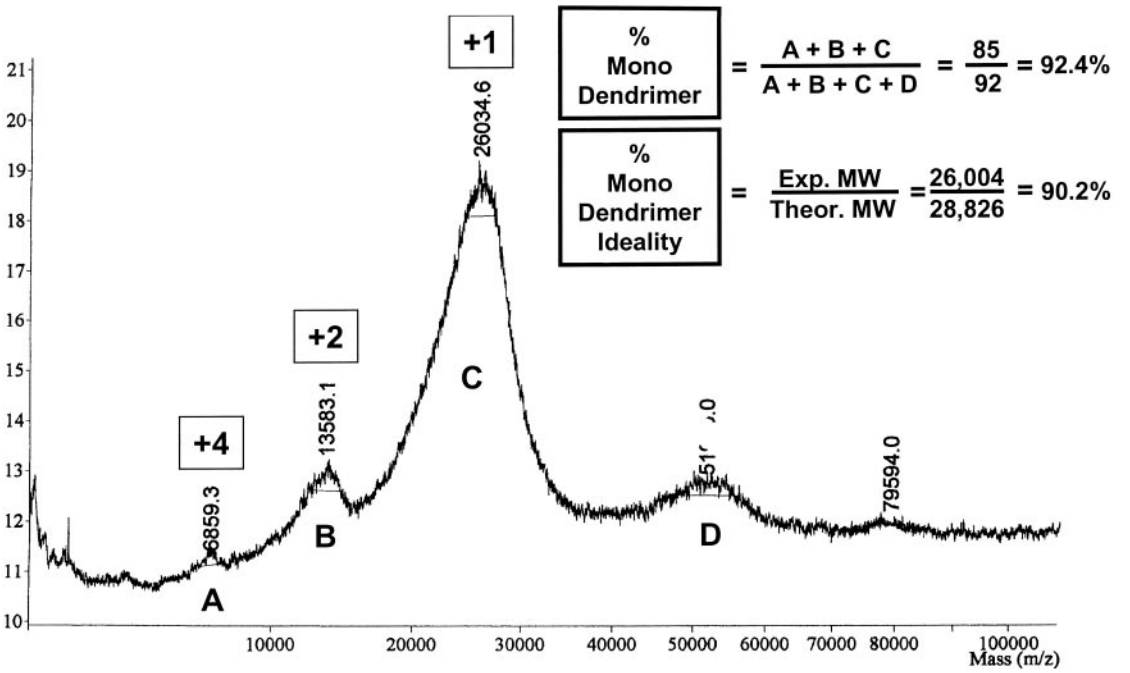

Fig. 3. A typical MALDI-TOF mass spectrum of [EDA]-*dendri*-{PAMAM-(G = 5.0)-NH_{128}}, wherein *A* is the parent ion + 1 species accompanied by *B* = +2 and *C* = +4 species. A small amount of dimer (*D*) (10%) is noted and corroborated by PAGE densitometer measurements.

by SEC indicated the presence of high MW product equivalent to a G = 7 PAMAM dendrimer in size (i.e., MW = 116,493). This was confirmed by PAGE analysis, which indicated a molecular mass of 116,000 Da (Fig. 5).

Pacification reactions. The above product was added to a mixture of anhydrous K_2CO_3 (2.3 g, 16.5 mmol), Tris(2-hydroxymethyl) aminomethane (2.0 g, 16.5 mmol), and 10 ml of MeOH. This mixture was stirred for 18 h at 25°C. The resulting mixture was diafiltered in 100 ml of deionized water by using an Amicon 30,000 MW cutoff, regenerated cellulose membrane followed by ultrafiltration to give a total of 8 liters of permeate. Removal of the (Tris) pacified product was monitored by SEC. This mixture was filtered, stripped of volatiles on a rotary evaporator at 2.8 in Hg at 60°C, and dried under high vacuum overnight to give 150 mg of white solid product. A MALDI-TOF-MS of this material indicated a peak molecular mass of 120,026 Da (see Table 1).

Synthesis: Route II—Reaction of [[EDA];PAMAM, G = 4.5; -$(CO_2Me)_{128}$] with Excess {[EDA];PAMAM, G = 3.0; -$(NH_2)_{32}$ } → [D_c -E-Y]-*amide*-{D_s-N-X}$_n$; Compound 5. *Autoreactive (PS:CST) product.* To a 50 ml one neck round bottom containing a stir bar was added {[EDA]; PAMAM, G = 3.0; -$(NH_2)_{32}$} (8 g, 1.16 mmol 100 equivalents per PAMAM dendrimer, G = 4.5) dissolved in 16 g MeOH followed by the addition of anhydrous lithium chloride (280 mg, 4 equivalents per ester). While stirring under N_2 and cooling at 0–5°C, the core reagent [[EDA];PAMAM, G = 4.5; -$(CO_2Me)_{128}$] (264 mg, 1.05 × 10^{-5} mol) dissolved in 2 g of MeOH was added. This mixture was allowed to warm to room temperature and placed in a bath at 40°C. The flask was sealed and heated under N_2 for 25 days with stirring, while monitoring periodically for completion by SEC and PAGE analysis. The resulting mixture was cooled to 25°C and opened under N_2. Analysis of the crude reaction mixture, after partial removal of excess shell reagent by ultrafiltration, gave a product with molecular mass of 114,500 Da (see Table 2). Attempts to isolate this product by further ultrafiltration and solvent removal led to rapid formation of very high MW products.

Pacification reaction. To this mixture was added ethanolamine (816 mg, 13.4 mmol, 10 equivalents per ester) in 1 g MeOH. After stirring for 6 days at 25°C, an Fourier transform IR spectrum of the crude mixture showed the complete absence of the PAMAM dendrimer ester carbonyl at 1,735 cm^{-1}. This mixture was ultrafiltered with a tangential flow ultrafiltration apparatus by using a 30-K MW cutoff membrane and deionized water. The purified mixture in deionized water was evacuated free of volatiles on a rotary evaporator and then dissolved in MeOH. It was redissolved in MeOH and devolatilized, and this sequence was repeated four times. Analysis of this material by SEC and PAGE indicated a monodispersed material. Analysis of an aliquot of the reaction mixture by PAGE, using a standard calibration curve derived from PAMAM dendrimers (G = 1–10), indicated a MW that corresponds to a PAMAM MW between G = 7 and G = 8 (i.e., MW ≅ 130,000) (Fig. 6).

Results and Discussion

The use of traditional divergent/convergent strategies for the synthesis of precise nanostructures (i.e., dendrons and dendrimers) larger than ≈15–20 nm has several serious disadvantages. First,

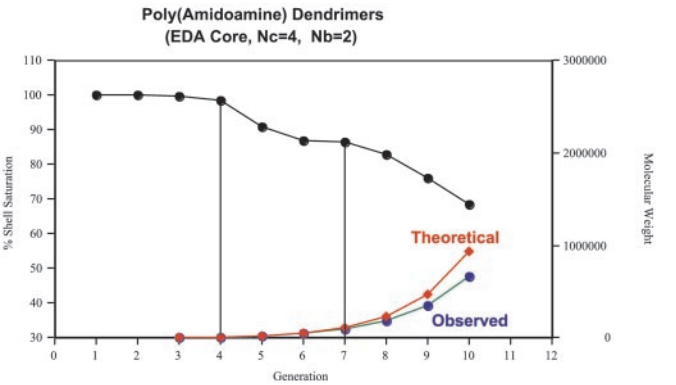

Fig. 4. Comparison of theoretical/observed MWs and % shell filling for [EDA] PAMAM dendrimers as a function of G = 1–10.

Table 1. PS pacified: CST; mass/shell-filling analysis

	Compound **1**	Compound **2**	Compound **3**	Compound **4**
Formula [D_c-N-Y]-*amide*-{D_s-E-Z}$_n$[†]	[D_c4Y]-*amide*-{D_s-2.5Z*}$_n$	[D_c5Y]-*amide*-{D_s-2.5Z**}$_n$	[D_c6Y]-*amide*-{D_s-3.5Z**}$_n$	[D_c7Y]-*amide*-{D_s-4.5Z**}$_n$
MW (calculated) for saturated shell[‡]	90,214	132,461	456,066	894,795
Number of shell tectons observed[§]/ theoretical[¶]	4/9	8–10/15	6–8/15	6/27
% Shell filling	44	53–66	40–53	40
MALDI-TOF-MS (MW)	56,496	120,026	227,606	288,970
PAGE (MW)	58,000	116,000	233,000	467,000
AFM observed dimensions	25 × 0.38 nm (D,H)	33 × 0.53 nm (D,H)	38 × 0.63 nm (D,H)	43 × 1.1 nm (D,H)
Calc (MW)[‖]	56,000	136,000	214,000	479,000

N, nucleophilic dendrimer core reagent; E, electrophilic dendrimer shell reagent; Z, surface group functionality; Z*, EA amide groups; Z**, *tris*-hydroxymethyl aminomethane amide groups.

[†]In the notation [D_c-N-Y]-*amide*-{D_s-E-Z}$_n$ above, n = number of dendrimer shell molecules {D_c-E-Z} surrounding the dendrimer core molecule [D_c-N-Y], where [D_c-N-Y] represents amine-terminated, [EDA], generation N, PAMAM dendrimer core reagent and {D_c-E-Z} represents carboxymethyl ester terminated, [EDA], generation E, PAMAM dendrimer shell reagent.

[‡]MW of theoretical number of shell dendrimer tectons plus core tecton, as determined from MALDI-TOF-MS data for individual core and shell tecton MWs. Values used for n in these calculations were obtained by using the Mansfield–Tomalia–Rakesh equation as described (48, 50).

[§]Based on the experimental MALDI-TOF-MS MWs of the tecto(dendrimer)s as isolated.

[¶]The theoretical number (n) of dendrimer shell molecules that would be expected to surround a specific dendrimer core molecule according to the Mansfield–Tomalia–Rakesh equation (48, 50).

[‖]Calculated MWs based on dome dimensions observed on a mica surface (46).

these strategies are hampered by the large number of reiterative synthetic steps required to attain these higher dimensions [e.g., PAMAM dendrimer (G = 9); diameter ≅ 10 nm; requires 18 reaction steps]. Second, these constructions are limited by the "de Gennes dense packing" phenomenon, which precludes ideal dendritic construction beyond certain limiting generations (20, 47). (See Fig. 4. Note a mass defect equivalent to 77% shell saturation level is observed for G = 9 caused by de Gennes dense packing.) For these reasons, our attention turned to the use of dendrimers as reactive modules for the rapid construction of controlled nanoarchitectures possessing higher complexity and dimensions beyond the dendrimer. We refer to these generic poly(dendrimers) as megamers (Fig. 1). Both randomly assembled megamers (49), as well as structure-controlled megamers (9, 46, 48) have been demonstrated. Recently, new mathematically defined megamers (dendrimer clusters) or SS:CST have been reported (9, 46, 48). The principles involved for the synthesis of these structure-controlled megamers mimic those used for the traditional core-shell construction of the basic dendrimer modules. First, a dendrimer core reagent is selected as a target substrate (i.e., usually a spheroid). Next, a limited amount of the reactive core reagent is combined with an excess of a dendrimer shell reagent. The objective is to completely saturate the target spheroid surface with covalently bonded dendrimer shell reagent. Because the diameters of the dendrimer core and shell reagents are very well defined, it is possible to mathematically predict the number of dendrimer shell molecules required to saturate a targeted dendrimer core (48, 50).

These relationships were analyzed mathematically as a function of core (r_1) and shell (r_2) radii ratios (50). At low r_1/r_2 values (i.e., 0.1–1.2) very important symmetry properties emerge as shown in Fig. 7. It can be seen that when the core reagent (r_1) is small and the shell reagent (r_2) is larger, only a very limited number of shell-type dendrimers can be attached to the core dendrimer based on available space. However, when the ratio of core radius to shell radius is equal to or greater than 1.2, space becomes available to attach many more shell reagents up to a discrete saturation level. The saturation number (*N max*) is well defined and can be predicted from a general expression that is described by the Mansfield–Tomalia– Rakesh equation (Fig. 7).

Dendrimer surfaces are amply endowed with polyvalent, exopresentations of chemical functionality and as such function as unique templates upon which to perform a wide variety of supramolecular chemistry. In fact, supramolecular self-assembly of simple electrophilic and nucleophilic reagents have been implicated in the very act of constructing basic PAMAM dendrimers generation by generation (11). Therefore, it is appropriate to speculate that such related supramolecular events may occur by means of polyvalent enhanced interactions at juxtapositioned dendrimer surfaces in these present core-shell constructions. Charge neutralized self-assembly of dendrimer core and shell reagents to produce

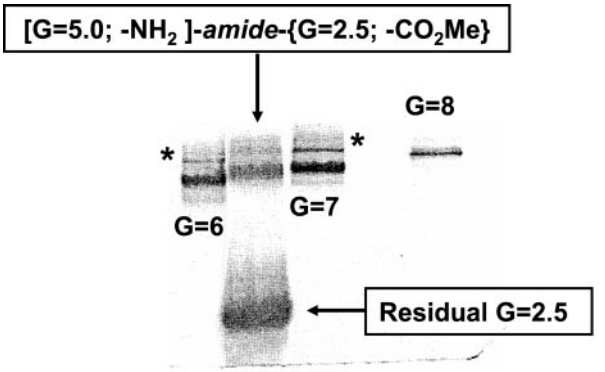

Fig. 5. PAGE analysis of [G = 5.0; -NH_2]-*amide*-{G = 2.5, -CO_2Me} core-shell tecto (dendrimer) prepared by Route I. This product is compared with PAMAM dendrimer tectons (G = 6, 7, and 8) containing their respective dimers (*).

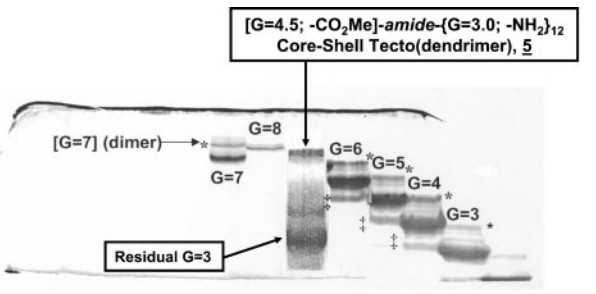

Fig. 6. Page analysis of [G = 4.5; -CO_2Me]-*amide*-{G = 3.0; -NH_2}$_{12}$ core-shell tecto(dendrimer) **1** prepared by Route II. This product is compared with PAMAM dendrimer tectons (G = 3–8) containing their respective dimers (*) and precursor generations (‡) (i.e., G-1).

Table 2. PS reactive: CST; mass/shell filling analysis

	Compound **5**	Compound **6**	Compound **7**	Compound **8**
Formula [D_c-E-Y]-*amide*-{D_s-N-X}$_n$†	[D_c4.5Y]-*amide*-{D_s3.0X}$_n$*	[D_c4.5Y]-*amide*-{D_s3.0X}$_n$**	[D_c4.5Y]-*amide*-{D_s4.0X}$_n$*	[D_c4.5Y]-*amide*-{D_s5.0X}$_n$*
MW (calculated) for saturated shell‡	173,915	140,133	202,352	255,847
Number of shell tectons observed§/ theoretical¶	12/21	14/23	3–4/12‖	2–3/8††
% Shell filling	65	62	36	33
PAGE (MW)	114,500	87,340	73,500	84,000

†In the notation [D_c-E-Y]-*amide*-{D_s-N-X}$_n$, n = number of dendrimer shell molecules {D_s-N-X} surrounding the dendrimer core molecule [D_c-E-Y], where [D_c-E-Y] represents carboxymethyl ester-terminated, [EDA* or NH_3**], generation E, PAMAM dendrimer core reagent and {D_s-N-X} represents amine-terminated, [EDA* or NH_3**] core, generation N, PAMAM dendrimer shell reagent.

‡MW of theoretical number of shell dendrimer tectons plus core tecton, as determined from MALDI-TOF-MS data for individual core and shell tecton MWs. Values used for n in these calculations were obtained by using the Mansfield–Tomalia–Rakesh equation as described (48, 50), or when $r_1/r_2 < 1.2$ then ‖$r_1/r_2 = 1.1$ (shell saturation = 12), ††$r_1/r_2 = 0.72$ (shell saturations = 8).

§Based on the experimental PAGE MWs of the reactive tecto(dendrimer)s as observed in crude reaction mixture after partial removal of excess shell reagent.

¶The theoretical number (n) of dendrimer shell molecules that would be expected to surround a specific dendrimer core molecule according to the Mansfield–Tomalia–Rakesh equation or when $r_1/r_2 < 1.2$ (48, 50).

SS:CSTs possessing essentially homogenous surface topologies has been reported recently (48). Unlike the charge neutralized preassembly and annealing conditions used for preparing SS:CSTs, which yield high shell saturation products (i.e., 75–87%), the present strategies preclude conditions for such annealing events before covalent bond formation. As a consequence, inefficient, but reproducible, parking of dendrimer shell reagents on the limited, well-defined targeted core surfaces were expected to lead to lower shell saturation levels and differentiated surface topologies. We refer to these constructs as PS:CSTs.

PS:CST architectures exhibiting reactive cusp/cleft functionality combinations such as [D_c-N-X]-*amide*-{D_s-E-Y}$_n$ (Route I) and [D_c-E-Y]-*amide*-{D_s-N-X}$_n$ (Route II) have been synthesized as illustrated in Fig. 8. These core-shell constructs offer cusp/cleft surface topologies that are differentiated in nanoscale dimensions much as one would expect to find in globular protein complexes illustrated in Fig. 2. Such synthetic differentiated, nanoscale surfaces should allow future tailoring to a wide variety of size- and recognition-sensitive functionalities of interest to supramolecular chemists. The intention of this work is to present preliminary synthesis protocols for these structures and to compare the unique physio/chemical properties of these unsaturated core-shell architectures to their more benign undifferentiated SS:CST analogues, which we reported earlier (48).

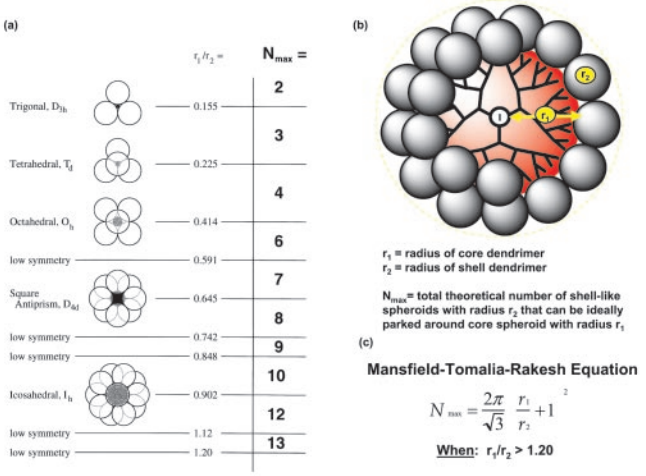

Fig. 7. (*a*) Symmetry properties for core-shell structures where $r_1/r_2 < 1.20$. (*b*) Sterically induced stoichiometry based on radii (r_1) and (r_2) core and shell dendrimers, respectively. (*c*) Mansfield–Tomalia–Rakesh equation for calculation of maximum shell filling when $r_1/r_2 > 1.20$ (48, 50).

Route I: Assembly of Electrophilic Dendrimer Shell Reagents Around a Nucleophilic Dendrimer Core. Under relatively mild, high dilution conditions in the presence of approximately 100 molar excesses of dendrimeric shell reagents, one can produce autoreactive PS:CSTs. Reactions leading to these products were monitored by SEC, capillary electrophoresis, MALDI-TOF MS, and PAGE. Higher MW species relative to reactants were observed to form and converge to relatively monodispersed products as typically observed by PAGE for PS:CST: [G = 5.0; -NH_2]-*amide*-{G = 2.5; -CO_2Me}$_{8-10}$ (Fig. 5). The monodispersity of these products was also confirmed by AFM (46). Attempts to reduce shell/core reagent ratios to 25- to 50-molar excesses, by either route, led to substantially poly(dispersed) products as determined by PAGE, MALDI-TOF MS, and capillary electrophoresis.

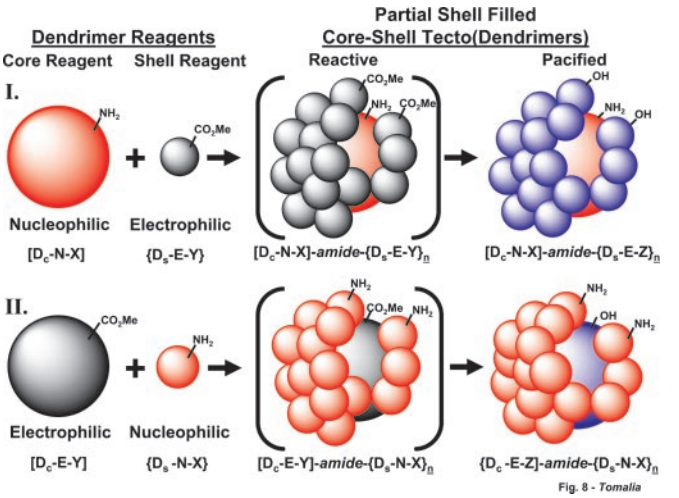

Fig. 8. Two routes to partial shell-filled tecto(dendrimers). Route I involves amidation of a limited amount of nucleophilic core dendrimer with an excess of electrophilic shell dendrimer reagent to produce reactive (PS:CST)-[D_c-N-X]-*amide*-{D_s-E-Y}$_n$. These products may be pacified by reacting with EA or Tris(hydroxymethyl) aminomethane (Tris) to produce shell-pacified-(PS:CST)-[D_c-N-X]-*amide*-{D_s-E-Z}$_n$. Route II involves amidation of a limited amount of electrophilic core dendrimer with an excess of nucleophilic shell dendrimer reagent to produce reactive-(PS:CST)-[D_c-E-X]-*amide*-{D_s-N-X}$_n$. These products may be converted to pacified forms by reacting with EA or an excess of EDA to produce core pacified-(PS:CST)-[D_c-E-Z]-*amide*-{D_s-N-X}$_n$.

Interruption of these reactions before reaching the typical convergent monodispersed partial shell-filled level (i.e., before 30 days/40°C) revealed populations of low shell saturation level products. Removal of excess shell reagents by ultrafiltration at these stages yielded very intractable products that readily transformed into gels and higher MW clusters.

Transformations by Route I (Fig. 8) would be expected to yield products with a reactive cusp/cleft functionality motif possessing a predominance of carboxymethyl ester cusps and a background of primary amine clefts. In general, these unpacified products were found to be more robust and resistant to MW building cascades than the reverse, reactive cusp/cleft functionality combinations expected from Route II (i.e., [D_c-E-Y]-*amide*-{D_s-N-X}$_n$).

Reactive cusp/cleft precursors to pacified compounds **1**-**4** (i.e., [D_c-N-X-]-*amide*-{D_s-E-Y}$_n$; Table 1), could in general be isolated as white cream-colored solids. This was possible after ultrafiltration and subsequent solvent removal under mild, high vacuum conditions. However, attempts to store these products even at low temperature in the solid state (i.e., <0C°) resulted in conversions to high MW clusters/gels.

Various amine-terminated PAMAM dendrimers were used as core reagents (i.e., G = 4, 5, 6, and 7-NH_2 terminated) in combination with several methyl ester-terminated PAMAM dendrimers (i.e., G = 2.5, 3.5, and 4.5 carboxymethyl esters), which were used as shell reagents. Generally, large excesses of shell reagent (i.e., 100× molar excess) were combined with a limited amount of core reagent in a sealed tube and heated at 40°C for 25 days. The reactions were monitored by Fourier transform IR spectroscopy, ^{13}C-NMR, SEC, and PAGE. Conversions to the core-shell tecto-(dendrimer) products were followed by observing the appearance of higher MW (i.e., shorter retention time products) by using SEC. Additional evidence was gained by observing the loss of reactant dendrimer bands on PAGE gels accompanied by the appearance of relatively monodispersed higher MW product bands. Removal of solvent gave solid, white metastable products. Either heating or allowing these solid products to stand at room temperature or even reduced temperatures (i.e., 0°C) led to polydispersed dendrimer cluster/gel formation. One could perform MW measurements by using SEC or PAGE by ultrafiltering excess shell reagent from the higher MW covalent dendrimer cluster products, providing samples were not taken to dryness. A typical PAGE analysis produced relatively tight product bands that were compared with a MW calibration curve derived from a standardized series of PAMAM dendrimers (i.e., G = 2–10) (Fig. 5).

Evidence supporting the reactive cusp/cleft topologies (Fig. 8) was garnered by performing appropriate pacification reactions on the respective electrophilic cusps or clefts resulting from Routes I and II. Preferred reagents for this task included the use of 2-aminoethanol (EA) or Tris in slight excess. These pacification reactions were monitored by following the complete disappearance of ester bands at 1,734 cm^{-1} by using Fourier transform IR spectroscopy. The resulting products, compounds **1**-**4** (Table 1), were isolated as robust, relatively monodispersed, solvent soluble, white solids that were very benign to MW building reactions even in the solid state. As shown in Fig. 8, the carbomethoxy ester groups residing at the termini of the attached shell reagents were amidated and now terminated with nonreactive hydroxyl groups.

Extensive characterization by AFM showed that these products were indeed monodispersed spheroids that were consistent with size enhancements that one might expect from various core and shell combinations (46). A distinct core-shell dimensional enhancement was observed as a function of the sum of the core and shell generation values of the reagents used in the construction of this series (e.g., Table 1, compound **1** > **2** > **3** > **4**). MWs for these products were determined by MALDI-TOF-MS and PAGE. They were corroborated by experimental AFM dimension values. These values were used in empirical MW calculations that were based on the observed property that all of the PS:CST products in this series

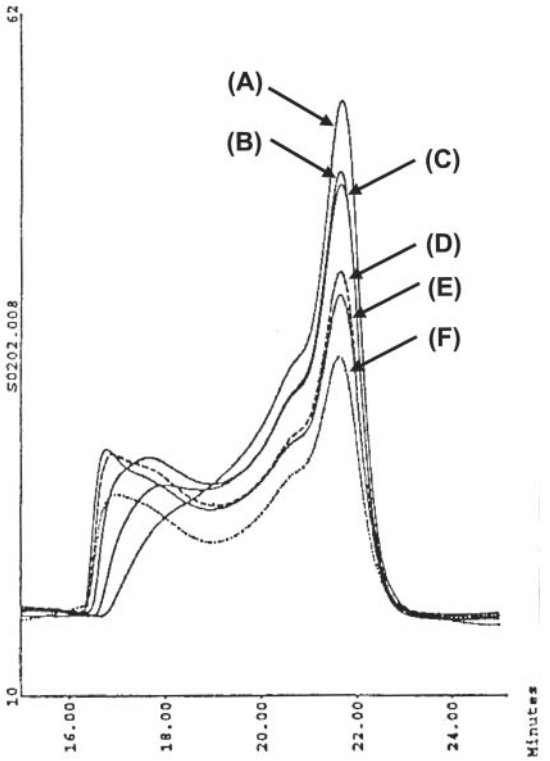

Fig. 9. SEC elutograms monitoring conversion of (PS:CST) [G = 4.5-CO_2Me]-*amide*-{G = 5.0; -NH_2}$_n$ into higher MW product cascade upon prolonged heating. PS:CST product isolated by ultrafiltration after allowing reaction to proceed 17 days at 40°C (*A*). Prolonged refluxing in methanol for (*B*) 2 days, (*C*) 4 days, (*D*) 6 days, (*E*) 8 days, and (*F*) 10 days.

were very deformable structures that could be measured as nearly perfect domes on mica surfaces (46) (Table 1).

Based on experimentally determined MWs, one can estimate the extent of shell filling by comparing these experimental MW values with mathematically predicted saturated levels calculated from the r_1 and r_2 values of the respective core and shell reagents (48, 50). Such a comparison indicated a shell filling range of 40% to 66% for this series.

Route II: Assembly of Nucleophilic Dendrimer Shell Reagents Around an Electrophilic Dendrimer Core. *Autoreactive (PS:CST) products.* Carboxymethyl ester-terminated PAMAM dendrimers were targeted as core reagents (i.e., G = 4.5; -CO_2Me terminated), whereas, various amine-terminated PAMAM dendrimers (i.e., G = 3.0, 4.0 and 5.0; = -NH_2 terminated) were combined in excess as shell reagents. Generally, large excesses of shell reagent (i.e., 100× molar excesses in methanol) were allowed to react with a limited amount of core reagent in a sealed tube by heating at 40°C for 25 days. Progress of the reactions was monitored by ^{13}C/^{1}H-NMR, SEC, PAGE, and Fourier transform IR spectroscopy. Following the disappearance of the core reagent methyl ester peak by ^{1}H-NMR indicated the reactions proceeded rather slowly, even under these conditions. The loss of ester functionality was observed to level off at 40% after 17 days. Analysis by SEC and PAGE revealed higher MW products relative to reactants (46). These higher MW products were remarkably monodispersed as determined by SEC, PAGE, and an independent study using AFM. Essentially identical results were obtained for both [EDA] and [NH_3] core dendrimer reactants (compare **5** and **6**, Table 2). Attempts to isolate the reactive forms of these products by solvent removal, invariably led to MW building events.

The autoreactive cusp/cleft (PS:CST) surfaces (i.e., [D_c-E-Y]-*amide*-{D_s-N-X}$_n$) obtained by Route II were substantially less stable to isolation than those reactive analogues produced by Route I. These differentiated surfaces (i.e., compounds **5–8**, Table 2) readily converted to high MW cascade products upon attempts to remove solvent, heating, or prolonged standing in solution at room temperature (i.e., >6–8 months). Efforts to selectively catalyze the amidation reaction between the core and shell reagent by use of cyanide ion enhanced the reaction rate dramatically; however, concurrent conversion to higher MW products could not be avoided. It was possible to monitor these MW enhancement processes by SEC as illustrated in Fig. 9.

Autoreactive PS:CST products obtained under noncatalyzed conditions were found to be relatively monodispersed with shell filling values ranging from 38% to 65% (Table 2).

Pacified (PS:CST) products. Pacification of reactive (PS:CST) obtained by Route II (i.e., compound **5**) was demonstrated by reaction with a 10-fold ester equivalent excess of EA and conversion to the pacified form (i.e., [D_c-E-Z-]-*amide*-{D_s-N-X}$_n$, where Z = EA, Fig. 8). Complete amidation of the residual core reagent ester groups was observed by following the disappearance of ester carboxylate at 1,735 cm^{-1}. The resulting white solid products obtained after ultrafiltration and devolatilzation were stable and resistant to MW building reactions.

Conclusions

Synthetic procedures are presented for two approaches to covalent, structure-controlled dendrimer clusters that exhibit chemical and physical properties consistent with differentiated surface topologies as illustrated in Fig. 8. These constructs are referred to as PS:CSTs. One approach (Route I) produces autoreactive electrophilic cusps and nucleophilic clefts, whereas the alternate route (Route II) yields autoreactive nucleophilic cusps and electrophilic clefts. The physical and chemical properties for these two series differ substantially from previously reported SS:CSTs. Chemical behavior of the unpacified forms of these differentiated architectural types strongly suggest that reactive, differentiated cusps and clefts are intrinsic features of these partial shell-filled dendrimer clusters. These reactive kinetic products are readily transformed into more thermodynamically stable poly(clusters) and gels upon heating or solvent removal. Simple amidation reactions that convert either the electrophilic carbomethoxy ester cusps or clefts into nonelectrophilic surface groups successfully pacify these core-shell structures against MW building, cluster/gelation reactions.

In summary, this work demonstrates that surface-differentiated reactivity associated with unfilled shells in core-shell architecture prevails at higher levels of complexity beyond the fundamental dendrimer core-shell structures. This completes a pattern that was first recognized by one of us (D.A.T.) for basic dendrimer modules in 1993–1994 (19). In this earlier work, it was noted that if fundamental core-shell dendrimer structures were not shell-saturated to complete mathematically predicted saturation levels the resulting branch shell-differentiated structures were metastable and very prone to participate in autoreactive, MW building cascade reactions. As shown in this present work, analogous shell unsaturated tecto-(dendrimer) structures exhibit autoreactivity unless pacified. In contrast, saturated shell tecto(dendrimers) attaining mathematically predictable saturation levels are well known to be robust and inert toward such autoreactivity (48). One must ask this important question: could it be possible that reactivity patterns observed for these two present molecular-level core-shell systems represent abstract mimics of reactivity patterns observed at the atomic level?

We are grateful to Dr. G. L. Hagnauer for valuable discussions and support. We express deep appreciation to Ms. L. S. Nixon for manuscript preparation. This work was funded by the Army Research Laboratory Dendritic Polymer Center of Excellence (Contract DAAL-01-1996-02-044).

1. Eigen, M. (1971) *Naturwissenschaften* **10,** 465–473.
2. Eigen, M., Gardiner, W., Schuster, P. & Winkler-Oswatitsch, R. (1982) *Evolution Now* (Freeman, New York).
3. Kuhn, H. & Waser, J. (1981) *Angew. Chem. Int. Ed.* **20,** 500–520.
4. Prigogine, I. (1972) *Physics Today* **25,** 38–44.
5. Mason, S. F. (1991) *Chemical Evolution* (Clarendon, Oxford).
6. Lehn, J. M. (1995) *Supramolecular Chemistry, Concepts, and Perspectives* (VCH, Weinheim).
7. Whitesides, G. M., Mathias, J. P. & Seto, C. T. (1991) *Science* **254,** 1312–1319.
8. Goodsell, D. S. (2000) *Am. Sci.* **88,** 230–237.
9. Tomalia, D. A., Uppuluri, S., Swanson, D. R. & Li, J. (2001) *Pure Appl. Chem.* **72,** 2343–2358.
10. Tomalia, D. A. & Frechet, J. M. J. (2001) in *Dendrimers and Other Dendritic Polymers*, eds. Fréchet, J. M. J. & Tomalia, D. A. (Wiley, West Sussex), pp. 631–633.
11. Tomalia, D. A. & Majoros, I. (2000) in *Supramolecular Polymers*, ed. Ciferri, A. (Dekker, New York), pp. 359–434.
12. Tomalia, D. A., Baker, H., Dewald, J., Hall, M., Kallos, G., Martin, S., Roeck, J., Ryder, J. & Smith, P. (1985) *Polym. J.* **17,** 117–132.
13. Fréchet, J. M. J. & Tomalia, D. A. (2001) *Dendrimers and Other Dendritic Polymers*, (Wiley, West Sussex).
14. Tomalia, D. A. (1995) *Sci. Am.* **272,** 62–66.
15. Newkome, G. R., Moorfield, C. N. & Vögtle, F. (1996) *Dendritic Molecules* (VCH, Weinheim).
16. Fréchet, J. M. J. (1994) *Science* **263,** 1710–1715.
17. Zeng, F. & Zimmerman, S. C. (1997) *Chem. Rev.* **97,** 1681–1712.
18. Matthews, O. A., Shipway, A. N. & Stoddard, J. F. (1998) *Prog. Polym. Sci.* **23,** 1–56.
19. Tomalia, D. A. (1994) *Adv. Mater.* **6,** 529–539.
20. Lothian-Tomalia, M. K., Hedstrand, D. M. & Tomalia, D. A. (1997) *Tetrahedron* **53,** 15495–15513.
21. Kallos, G. J., Tomalia, D. A., Hedstrand, D. M., Lewis, S. & Zhou, J. (1991) *Rapid Commun. Mass Spectrom.* **5,** 383–386.
22. Dvornic, P. R. & Tomalia, D. A. (1995) *Macromol. Symp.* **98,** 403–428.
23. Tomalia, D. A. & Durst, H. D. (1993) in *Supramolecular Chemistry I: Directed Synthesis and Molecular Recognition*, ed. Weber, E. W. (Springer, Berlin), pp. 193–313.
24. Hummelen, J. C., van Dongen, J. L. J. & Meijer, E. W. (1997) *Chem. Eur. J.* **3,** 1489–1493.
25. Brothers, H. M., II, Piehler, L. T. & Tomalia, D. A. (1998) *J. Chromatogr. A* **814,** 233–246.
26. Zhang, C. & Tomalia, D. A. (2001) in *Dendrimers and Other Dendritic Polymers*, eds. Fréchet, J. M. J. & Tomalia, D. A. (Wiley, West Sussex), pp. 239–252.
27. Li, J., Piehler, L. T., Qin, D., Baker, J. R., Jr. & Tomalia, D. A. (2000) *Langmuir* **16,** 5613–5616.
28. Turro, N. J., Chen, W. & Ottaviani, M. F. (2001) in *Dendrimers and Other Dendritic Polymers*, eds. Fréchet, J. M. J. & Tomalia, D. A. (Wiley, West Sussex), pp. 309–330.
29. Watkins, D. M., Sayed-Sweeet, Y., Klimash, J. W., Turro, N. J. & Tomalia, D. A. (1997) *Langmuir* **13,** 3136–3141.
30. Esfand, R. & Tomalia, D. A. (2001) *Drug Discovery Today* **6,** 427–436.
31. Hecht, S. & Fréchet, J. M. J. (2001) *Angew. Chem. Int. Ed.* **40,** 74–91.
32. Kukowska-Latallo, J. F., Bielinska, A. U., Johnson, J., Spindler, R., Tomalia, D. A. & Baker, J. R., Jr. (1996) *Proc. Natl. Acad. Sci. USA* **93,** 4897–4902.
33. Ottaviani, M. F., Sacchi, B., Turro, N. J., Chen, W., Jockush, S. & Tomalia, D. A. (1999) *Macromolecules* **32,** 2275–2282.
34. Weener, J.-W., Baars, M. W. P. L. & Meijer, E. W. (2001) in *Dendrimers and Other Dendritic Polymers*, eds. Fréchet, J. M. J. & Tomalia, D. A. (Wiley, West Sussex), pp. 387–424.
35. Goodson, T., III (2001) in *Dendrimers and Other Dendritic Polymers*, eds. Fréchet, J. M. J. & Tomalia, D. A. (Wiley, West Sussex), pp. 515–541.
36. Bosman, A. W., Janssen, H. M. & Meijer, E. W. (1999) *Chem. Rev.* **99,** 1665–1688.
37. Percec, V., Johansson, G., Ungar, G. & Zhou, J. P. (1996) *J. Am. Chem. Soc.* **118,** 9855–9866.
38. Percec, V., Ahn, C.-H., Unger, G., Yeardly, D. J. P. & Moller, M. (1998) *Nature (London)* **391,** 161–164.
39. Hudson, S. D., Jung, H.-T., Percec, V., Cho, W.-D., Johansson, G., Ungar, G. & Balagurusamy, V. S. K. (1997) *Science* **278,** 449–452.
40. Sayed-Sweet, Y., Hedstrand, D. M., Spindler, R. & Tomalia, D. A. (1997) *J. Mater. Chem.* **7,** 1199–1205.
41. Karp, G. (1984) *Cell Biology* (McGraw–Hill, New York).
42. Tomalia, D. A., Baker, H., Dewald, J., Hall, M., Kallos, G., Martin, S., Roeck, J., Ryder, J. & Smith, P. (1986) *Macromolecules* **19,** 2466–2468.
43. Esfand, R. & Tomalila, D. A. (2001) in *Dendrimers and Other Dendritic Polymers*, eds. Fréchet, J. M. J. & Tomalia, D. A. (Wiley, West Sussex), pp. 587–604.
44. Smith, P. B., Martin, S. J., Hall, M. J. & Tomalia, D. A. (1987) in *Applied Polymer Analysis Characterization*, ed. Mitchell, J., Jr. (Hanser, Munich), pp. 357–385.
45. Tomalia, D. A., Naylor, A. M. & Goddard, W. A., III (1990) *Angew. Chem. Int. Ed. Engl.* **29,** 138–175.
46. Li, J., Swanson, D. R., Qin, D., Brothers, H. M., II, Piehler, L. T., Tomalia, D. A. & Meier, D. J. (1999) *Langmuir* **15,** 7347–7350.
47. de Gennes, P. G. & Hervet, H. J. (1983) *J. Phys. Lett.* **44,** 351–360.
48. Uppuluri, S., Piehler, L. T., Li, J., Swanson, D. R., Hagnauer, G. L. & Tomalia, D. A. (2000) *Adv. Mater.* **12,** 796–800.
49. Tomalia, D. A., Hedstrand, D. M. & Wilson, L. R. (1990) in *Encylopedia of Polymer Science and Engineering* (Wiley, New York), 2nd Ed., pp. 46–92.
50. Mansfield, M. L., Rakesh, L. & Tomalia, D. A. (1996) *J. Chem. Phys.* **105,** 3245–3249.